Impact of Temperature on Host-Parasite Interactions and Metabolomic Profiles in the Marine Diatom Coscinodiscus granii

Ruchicka Annie O'Niel , Georg Pohnert , Marine Vallet *

Posted Date: 31 October 2024

doi: 10.20944/preprints202410.2463.v1

Keywords: Bloom-forming algae; Diatoms; Parasitoid oomycete; Lagenisma coscinodisci; Host-parasite interactions; UHPLC-HRMS; Untargeted metabolomics; Temperature increase

Article

Impact of Temperature on Host-Parasite Interactions and Metabolomic Profiles in the Marine Diatom *Coscinodiscus granii*

Ruchicka O'Niel [1,2], Georg Pohnert [1,2] and Marine Vallet [1,2,*]

[1] Institute for Inorganic and Analytical Chemistry, Friedrich Schiller University Jena, Germany
[2] Max Planck Fellow Group Plankton Community Interaction, Max Planck Institute for Chemical Ecology, Jena, Germany
* Correspondence: mvallet@ice.mpg.de

Abstract: Diatoms are single-celled photosynthetic eukaryotes responsible for CO_2 fixation and primary production in aquatic ecosystems. The cosmopolitan marine diatom *Coscinodiscus granii* can form seasonal blooms in coastal areas and interact with various microorganisms, including the parasitic oomycete *Lagenisma coscinodisci*. This unicellular eukaryote is mainly present in the northern hemisphere as an obligate parasite of the genus *Coscinodiscus.* Understanding the interplay of abiotic factors such as temperature and biotic factors like parasitism on algal physiology is crucial as it dictates plankton community composition and is especially relevant in climate change. This study investigates the impact of two temperatures, 13°C and 25°C, on *Coscinodiscus granii* under laboratory conditions. A decreased infection rate of the parasite was observed at the elevated temperature. Comparative metabolomic analysis using UHPLC-HRMS revealed that temperature and parasitism significantly affect the algal metabolome. Abundances of metabolites related to sulfur metabolism, including cysteinoleic acid and dimethylsulfoniopropionate, as well as molecules linked to fatty acid metabolism, e.g., carnitine, acetylcarnitine, and eicosapentaenoic acid, significantly increase in cells grown at a higher temperature, suggesting the enhanced rate of metabolism of host cells as temperature rises. Our study reveals how temperature-induced metabolic changes can influence host-parasite dynamics in a changing climate.

Keywords: bloom-forming algae; diatoms; parasitoid oomycete; *Lagenisma coscinodisci*; host-parasite interactions; UHPLC-HRMS; untargeted metabolomics; temperature increase

1. Introduction

Phytoplankton comprises microalgae, such as diatoms and cyanobacteria, that form the basis of the marine food webs. The algae grow by interacting with diverse microorganisms, which creates the observable population dynamics of algal blooms [1]. Microalgae and their associated symbiotic microbes exchange chemical cues that regulate host physiology, metabolism, and defense [2–4]. The region surrounding phytoplankton cells where chemical exchanges occur is the phycosphere, which can attract many opportunists and microbial pathogens such as eukaryotic parasites [5]. Diverse microbial parasites targeting the group of diatoms and dinoflagellates can contribute to the termination of algal blooms in coastal ecosystems [6,7]. Parasites also play an essential role in bloom dynamics and ocean ecosystems [8], yet the impact of climate warming on their ecology and virulence remains poorly understood. The molecular patterns associated with the thermal adaptation of the parasites and the hosts need to be characterized if predictions on the future ocean system's functioning are made [9]. Climate changes, including temperature increases, can induce complex restructuring of the plankton community, impacting metabolic activities and the productivity of aquatic microorganisms in a hitherto only incompletely understood interaction framework [10].

Environmental conditions and abiotic factors such as temperature, pH, nutrient availability, and salinity modulate the physiology of microalgae in interactions and influence the behavior of aquatic

 doi:10.20944/preprints202410.2463.v1

pathogens and parasites [11]. An increasing number of studies suggest that higher temperatures cause adverse effects on the fitness of plankton parasites [12,13], with some aquatic microorganisms unable to adapt to rising temperatures [14]. Specific populations of a given species can also perform better under parasite exposure than others at increasing temperatures, shaping the competition between aquatic organisms even after parasite decline [15].

Untargeted metabolomics using MS or NMR instruments can identify metabolites within algal cells and those released into the environment. These released metabolites can be exchanged with coexisting microbes, especially within the diffusion-limited region around algal cells, the phycosphere. Alkaloids from the ß-carboline family involved in regulating the parasite infection of the bloom-forming diatoms *Coscinodiscus granii* were identified using UHPLC-HRMS analysis [16]. Furthermore, using an LDI-HRMS instrument, low molecular weight metabolites can be identified in diatoms and dinoflagellates infected by eukaryotic parasites, including phaeophorbide *a* and dimethylsulfoniopropionate [17]. There has been progress in using metabolomics to explore the host response to parasite infection, both in terms of how parasites derive energy from hosts and how hosts can modify their metabolism to resist infection [18]. However, no studies address the metabolic processes during host-parasite interaction during temperature increase, even if such multifactorial situations will be the rule, not the exception.

Here, we investigate the metabolic profiles of diatom cultures exposed to different temperatures and parasite treatments. We selected the diatom species *Coscinodiscus granii*, which has unique morphology and biotechnological potential. *C. granii* is used in studying silicification and environmental adaptation and represents a versatile and valuable model for a wide range of studies in diatom biology, ecology, and applied nanotechnology research [19]. We recorded the cell abundance at two incubation temperatures, e.g., 13°C and 25°C. We performed an infection assay with the specialist parasitoid *Lagenisma coscinodisci,* which can control *Coscinodiscus* spp. bloom to test its infectivity under two different temperature conditions. We identify and discuss metabolic alterations in the cellular metabolome of *C. granii* upon temperature increase and parasite infection. This study provides metabolic information on the collective impact of increased temperature and parasite infection on the physiology and cell metabolism of bloom-forming diatoms.

2. Results

2.1. Impact of Temperature on Diatom Host Abundance and Parasite Infectivity

The diatom species *Coscinodiscus granii*, a cosmopolitan and bloom-forming diatom, was cultivated at two incubation temperatures, e.g., 13°C and 25°C, starting with the initial cell density of 5 cells mL^{-1}. We recorded the cell density over 29 days and highlighted that, in the early and exponential growth phase (Day 6 to Day 12), cell density was significantly higher in cultures grown at 25°C (Supplementary Figure S1). Using dense cultures of *C. granii* with an initial cell density of 200 cells mL^{-1}, we test whether the parasitoid oomycete *Lagenisma coscinodisci* infects the algal cells at the two incubation temperatures. *C. granii* was susceptible to *Lagenisma* infection, and infected cells were observed at both incubation temperatures in the parasite-treated samples (Figure 1a). In the parasite-treated cells, higher cell densities were recorded at 25°C compared to the 13°C treatment. The parasite infection rate was higher at the lower temperature (Figure 1b). In sum, the increased temperature does not eliminate the ability of the parasite *L. coscinodisci* to infect its host. However, it can influence the host *C. granii* and its ability to resist parasite infection. Our findings are based on the cell density measurement of diatoms, and infection rate measurements are based on observing infected cells harboring the sporangia of *L. coscinodisci* (late sporocyte phase). The infection phenotype excludes the other stages of infection, such as the trophocyte and early sporocyte phase of infection, as it is hard to distinguish using conventional light microscopy and can represent the aborted infection process in diatom cells.

 doi:10.20944/preprints202410.2463.v1

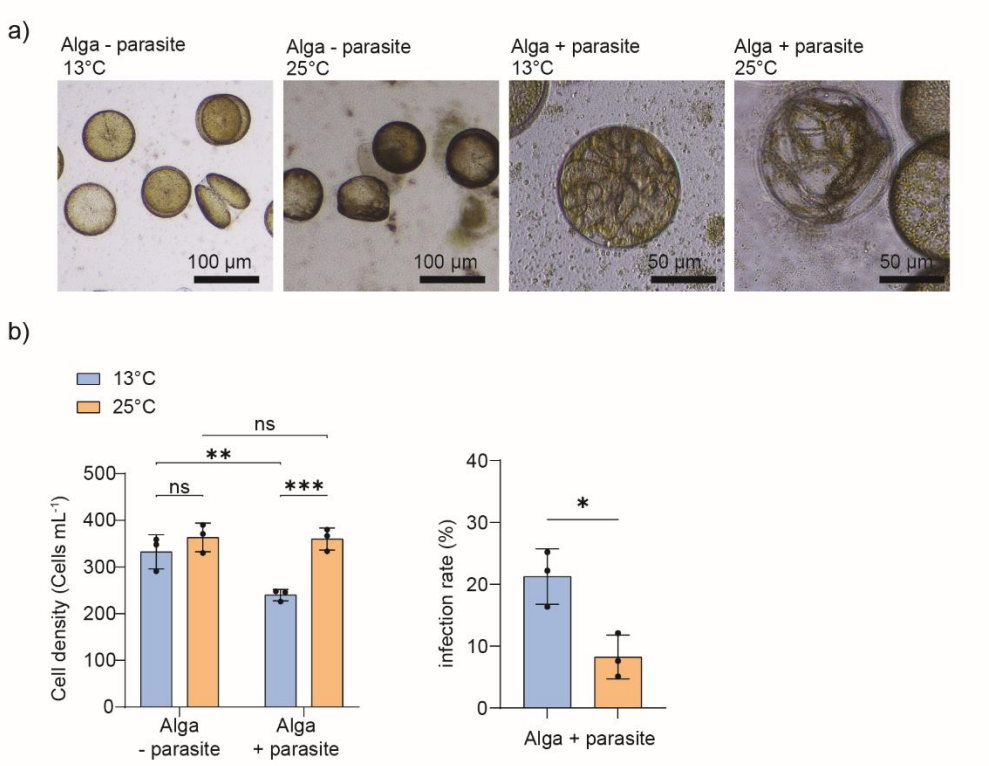

Figure 1. a) Microscopic pictures of *C. granii* cultures subjected to two incubation temperatures, 13°C and 25°C, and treated with the parasitic oomycete *L. coscinodisci* (Day 7). Infected cells harboring the parasite sporangia (late sporocyte phase) were observed at 13°C and 25°C. b) Monitoring of cell density of infected cells and infection rate in algal cultures of *C. granii* grown at 13°C and 25°C and inoculated or not with the parasite *L. coscinodisci* (+ or – parasite) (N = 3, 3 biological replicates). The statistical significance of cell abundance was tested with Two-Way ANOVA, and a *t*-test was conducted to compare infected cell density and infection rate at different temperatures (*** $p < 0.001$, ** $p < 0.01$, * $p < 0.05$, *ns* non-significant).

2.2. UHPLC-HRMS Analysis Reveals Altered Metabolome Patterns Associated with Different Temperatures and Parasite Infection in Diatom Cells

On day 7, 40 mL cultures from the above experiments were filtered, and the recovered alga cells were extracted with methanol. The extracts were dried and taken up with 80 µL of methanol before UHPLC-HRMS analysis. Chromatographic separation using C18 and ZIC-HILIC columns yielded two data matrices of 1,210 and 1,195 features, respectively. Features are characterized by a retention time, mass to charge (*m*/*z*) value, and peak intensity. After normalization based on the diatom cell counts, intensities were log-transformed and pareto-scaled. Principal component analysis (PCA) was conducted to reveal metabolic differences between algal cells grown at 13°C and 25°C and those treated or not with the parasite *L. coscinodisci* (NP: no parasite, WP: with parasite) (Figure 2). Significant discrimination was observed between all four groups, with a total explained variance of 79.8% and 68.8% for the profiling with C18 and ZIC-HILIC columns, respectively (Figure 2a-b). Metabolite variation driven by PC1 was related to higher temperature, while PC2 variation was associated with parasite treatment for the C18 dataset (Figure 2a). A few features were associated with parasite treatment, which could be explained by the low infection rates, which never reached over 20% (Figure 1b). A significant difference was thus mainly identified by algal metabolites up-regulated in cells grown at higher temperatures. Significant metabolites that drove these PCA were examined, and those that characterized cells grown in higher temperatures, regardless of the parasite treatment, were further identified using MS/MS analysis. Volcano plots were also inspected to search for and select significant features (Supplementary Figures S11-S16).

 doi:10.20944/preprints202410.2463.v1

Spectral similarity matching of the significant features was conducted with public databases using GNPS, and fragmentation analysis was done using SIRIUS:CSIFinger ID (Supplementary Figures S4-S10). The UHPLC-HRMS analysis using the ZIC-HILIC column facilitated the identification of a diverse range of polar and hydrophilic compounds (Supplementary Figure S2), such as serine, cysteinoleic acid, and dimethylsulfoniopropionate (DMSP), which were all significantly up-regulated in algal cells grown at 25°C (Figure 3a). These structures were confirmed with analytical standards (Supplementary Table S2). Furthermore, chemicals associated with fatty acid metabolism were also identified as more abundant in cells grown at 25°C, e.g., carnitine, acetylcarnitine, and eicosapentaenoic acid, and were confirmed with standards (Figure 3b). In the ZIC-HILIC dataset, two metabolites, ectoine, and the recently newly described 2-homoectoine were found and annotated based on spectral similarity matching of their MS/MS fragments with those of the public library. These two metabolites were not significantly regulated at 13°C but downregulated in parasite-treated cells compared to untreated algae at 25°C (Figure 3d).

Utilizing reverse-phase chromatography with a C18-column, we successfully identified two metabolites that discriminated between untreated algae grown at 13°C and those treated with the parasite *L. coscinodisci* (Supplementary Figure S3). Firstly, eicosapentaenoic acid, detected in positive polarity as *m/z* 303.2327 for $[M+H]^+$ at retention time of 8.2 min, and secondly, lumichrome, a riboflavin-derived metabolite, detected as *m/z* 243.0887 for $[M+H]^+$ at 3.7 min. Both metabolites were confirmed by co-injection studies with standards (Supplementary Figures S17-S18). Eicosapentaenoic acid (EPA) was detected in both parasite-treated and untreated cell metabolomes but with significantly higher abundance in untreated cells at both temperatures (Figure 3b). Eicosapentaenoic acid can underpin a modulation in lipid metabolism during parasitism [20,21]. Here, levels of EPA were significantly higher at 25°C but decreased in both temperature conditions under parasite treatment. Lumichrome is also significantly down-regulated in parasite-treated cells and is generally up-regulated in cells grown at 25°C (Figure 3c).

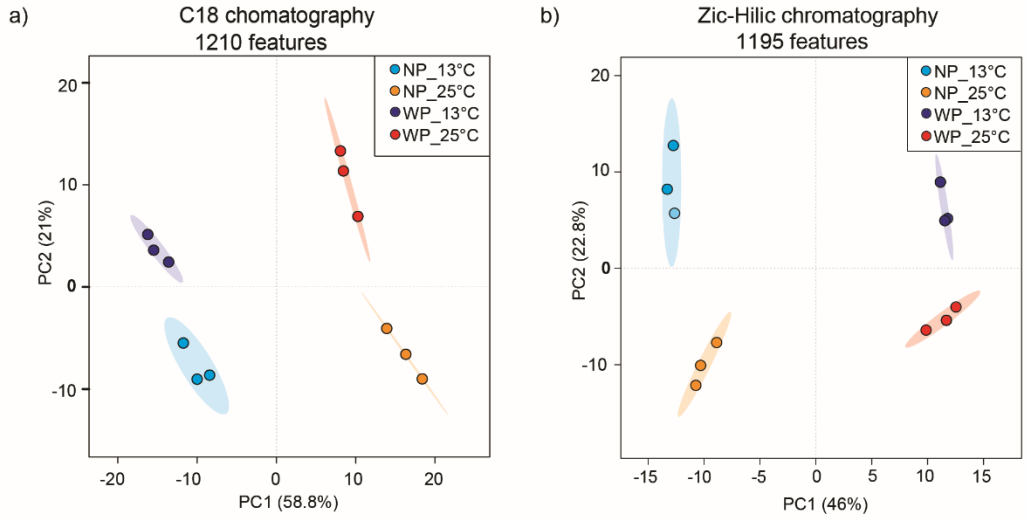

Figure 2. UHPLC-HRMS analysis using a) C18 and b) ZIC-HILIC chromatography discriminated metabolic profiles of the diatom *C. granii* cells treated with parasites (WP) as well as untreated cells (NP) incubated at 13°C and 25°C (N = 3, 3 biological replicates).

 doi:10.20944/preprints202410.2463.v1

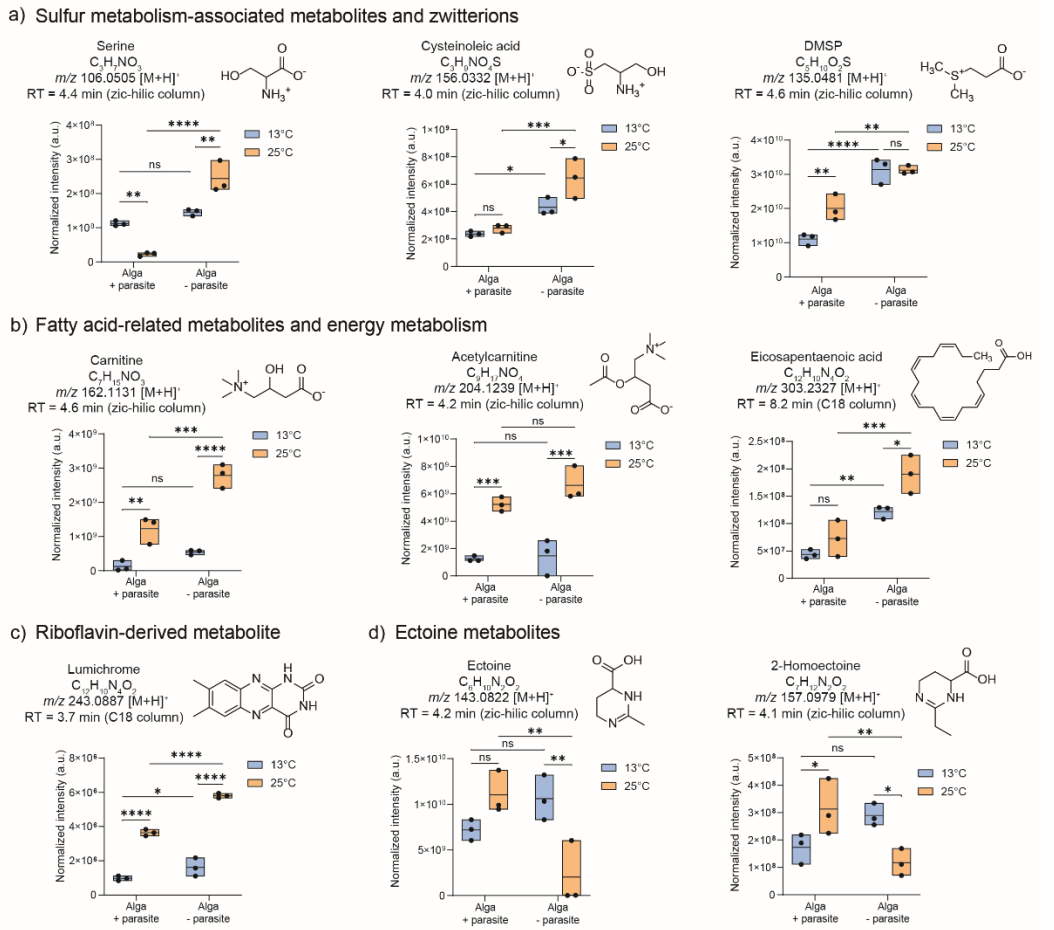

Figure 3. The identified compounds discriminated metabolic profiles of diatom *C. granii* cells treated with parasites (WP) from untreated samples (NP) incubated at 13°C and 25°C (N = 3, 3 biological replicates). Significant metabolites identified were from a) metabolites related to sulfur metabolism and zwitterions, b) metabolites involved in energy metabolism and related to fatty acids, c) riboflavin-derived lumichrome, and d) ectoine metabolites. The box plots display the maximum, minimum, and median lines, first/third quantiles, and the samples as points for the significant metabolites. Two-way ANOVA was conducted to achieve statistical significance using cell-based normalized intensities of the peaks (*** $p < 0.001$, ** $p < 0.01$, * $p < 0.05$, *ns* non-significant).

3. Discussion

3.1. Effect of Temperature on Cell Abundance of Bloom-Forming Diatom C. granii and Parasite Infectivity of L. coscinodisci

The bloom-forming diatom *Coscinodiscus granii* is an essential primary producer that inhabits the oceans. It is thereby subjected to environmental changes. Here, we recorded the effect of temperature on the algal cell abundance, cell metabolome, and parasite infectivity. The host and parasite strains were isolated in Helgoland waters during the bloom of November 2019, and water temperature usually ranges from 5 to 20°C over the year. For these potentially cold-adapted strains, 25°C might thus represent stress. However, high cell density was recorded for *C. granii* grown at 25°C, particularly in the exponential phase between 6 and 12 days of incubation and the late stationary phase after 25 days of incubation (Supplementary Figure S1). Cell density only remains higher at 13°C in the late exponential phase. Still, it could be likely that this alga can develop a bloom when young cells in the early growth phase are exposed to higher incubation temperatures. Previous reports have demonstrated that both *C. granii* and *L. coscinodisci* can be found in waters at the temperature range of 13°C to 20°C, with the percentage of infected cells ranging from 7.1% to 41.9% [22,23], which aligns with our present findings in laboratory experiments conducted at 13°C.

 doi:10.20944/preprints202410.2463.v1

We report that the parasitic oomycete *L. coscinodisci* can infect the diatom *C. granii*, regardless of the incubation temperature (Figure 1a-b). The number of infected cells was similar in cultures grown at both temperature regimes, but the infection rate, determined from the ratio of reproductive parasite cells (sporangia) and healthy cells, was significantly different (Supplementary Table S2). The infection rate was lower in algal cultures grown at 25°C compared to the 13°C treatment (Figure 1b). Therefore, *C. granii* might bloom with higher cell abundance, and the parasitic oomycete might be less efficient in infecting the algal population at higher temperatures. The number of reproductive parasite cells can also vary depending on the virulence of the parasite strains employed, which can influence the total cell density of cultures [24]. Previous literature suggests that aquatic parasite abundance might change according to temperature and host susceptibility to infection [9,15,25], and it would be interesting to test the effect of higher temperature on a broad strain spectrum of *L. coscinodisci* and other parasites targeting diatoms. Temperature plays a crucial role in the ocean ecosystem, and warmer waters can intensify stratification and shoaling of the upper mixed layer [26]. Some diatom species might tolerate a broad temperature spectrum, while others will thrive in a specific thermal niche [27].

The infection rate of the parasite *L. coscinodisci* never reached above 30% in laboratory experiments when cultured at 13°C and was even lower when cultured at 25°C (Figure 1b), which also follows the usual rates observed in the field during algal blooms [28]. The infection rates observed in our cultures are consistent with data from field observations that record that *L. coscinodisci* is present in natural blooms of *Coscinodiscus* at an infection rate of 5 to 47% [20]. We suggest that temperature may be just one factor influencing parasite infectivity, and algal resistance might be regulated by other means or factors.

3.2. Effect of Temperature on Cell Metabolic Profiles of the Bloom-Forming Diatom C. granii in Interaction with the Parasitic Oomycete

Diatoms exhibit adaptations to varying environmental temperatures, including adjustments in gene expression, membrane structure, and cellular metabolism [29]. Our metabolomics study indicates that temperature and parasite exposure impact diatom metabolic regulation in *C. granii* (Figure 2). We further observed key metabolic changes associated with temperature change that parasite exposure has also impacted. Multiple studies have demonstrated the influence of abiotic factors such as temperature on host-symbiont interactions. For instance, in marine macroalgae *Delisea pulchra*, host-pathogen interactions are temperature-dependent, with temperature-regulated production of furanones that prevent the infection by pathogenic bacteria *Ruegeria* sp. [30]. Similarly, studies on *Micromonas* sp. have shown that temperature can alter the viral lytic and lysogeny life cycle strategies of Prasinoviruses, potentially impacting ocean biogeochemistry [31]. Few compounds unique to the parasite-treated cells were detected in the present study, but the low infection rate might prevent the detection of subtle changes in the metabolome (Figure 1b).

Several algal metabolites were identified in the quality control pool sample with standards, including metabolites involved in sulfur- -metabolism, fatty acids metabolism, and riboflavin-derived substances (Figure 3, Supplementary Table S2). Reports have demonstrated that rising temperatures increase phytoplankton's DMSP and cysteinolic acid levels [32], which aligns with our findings in *C. granii* (Figure 3a). DMSP is produced in parasite-infected diatoms, although in lesser amounts than in non-infected cells (Figure 3), and might relate to *C. granii* susceptibility to *Lagenisma* oomycete. DMSP has been found as a marker of *Parvilucifera* parasites infecting the dinoflagellate *Alexandrium minutum* [17], and when hydrolyzed into dimethylsulfide, it can enable the parasite reproduction [33]. Although detected in lesser amounts in *Lagenisma*-treated diatom cells than in healthy cells (Figure 3), DMSP might also play a role in the diatom-oomycete interaction that has yet to be demonstrated. The role of DMSP in marine symbiotic interactions is well-documented. For example, in the relationship between the microalga *E. huxleyi* and the algicidal bacterium *Roseobacter* sp., the alga produces DMSP, which the microbe metabolizes and releases methanethiol [34]. Algal hosts with higher DMSP levels tend to be more susceptible to infection [34], potentially due to the attraction properties of this compound and its associated metabolites that are released [35]. In the

 doi:10.20944/preprints202410.2463.v1

coral *Pocillopora damicornis* and the pathogenic bacterium *Vibrio coralliilyticus*, the host secretes DMSP into its mucus, especially under high temperatures, attracting more pathogens and aiding disease progression during heat waves [36].

Cysteinolic acid is a sulfur-containing metabolite abundant in multiple phytoplankton species and is an adaptive strategy for high salinity stress [37]. This compound was detected as significantly abundant in untreated and parasite-treated cells grown at 25°C and might possess a role in alleviating the effect of temperature increase or during the host-parasite interaction. Ectoine and derivatives, including the recently newly described 2-homoectoine, are produced by marine algae and bacteria, and their abundance can increase in cells during salinity stress [38]. Here, parasite-treated cells display a reduced amount of ectoine, and no significant chances of an increase in incubation temperature were observed. This suggests that ectoine and derivatives might play a role in the host-parasite interactions but not in response to temperature stress.

Among the significantly up-regulated metabolites in cells grown at 25°C are three chemicals, we highlighted carnitine, acetylcarnitine, and EPA. In eukaryotes and microalgae, acetylcarnitines produce acetyl-CoA in plastids, which serve as a source of acetyl-CoA for fatty acid synthesis in the plastid [39]. Carnitine is essential for the transfer of fatty acids across the inner mitochondrial membrane and is also an osmolyte involved in the response to salinity stress in plants and microalgae [40], but its role in temperature stress and diatom-parasite interaction is not yet known. Here, we observed an increase of carnitine and acetylcarnitine with higher incubation temperature, regardless of the parasite treatment. It is also detected in all parasite-treated cultures (Figure 3b). In plants, fungal pathogenesis relies heavily on fatty acid metabolism, acetyl-CoA generation, and glyoxylate metabolism in the peroxisome, which is essential for pathogenesis, and this process, which depends on carnitine, may be conserved across terrestrial and aquatic habitats [41]. Eicosapentaenoic acid is a major fatty acid in diatoms and a precursor to many bioactive oxylipins [21]. Microalgae synthesize EPA primarily through aerobic metabolic pathways [42]. Nitrogen levels significantly influence EPA content. While low nitrogen boosts overall lipid production, the percentage of EPA decreases [43]. Nitrogen-replete conditions favor the production of EPA and polyunsaturated fatty acids in microalgae [44,45]. It has been theorized that high cell densities and cellular turnover could favor higher intracellular levels of EPA to maintain the membrane integrity of organelles in microalgae [46]. A slight increase in EPA levels during elevated temperatures could be tied to the enhanced cell growth rate observed for *C. granii*, especially in the early growth phase (Supplementary Figure S1). Intracellular parasites may also depend on the host's central carbon metabolism and lipids for fueling their development, replication, and propagation [47]. Additionally, EPA can be transformed to Polyunsaturated aldehydes (PUA) and other oxylipins that are not covered by our method but could potentially contribute to algal defense against parasite [47]. This might support our observations, indicating that parasite-treated cells of diatom *C. granii* are characterized by decreased levels of EPA.

Finally, lumichrome, a riboflavin derivative, has been detected in *C. granii* cells and is significantly up-regulated in both parasite-treated and untreated cells incubated at 25°C (Figure 3c). It was also detected in parasite-infected cells, although in lesser amounts. Here, we first report this compound's association with marine parasitic oomycete-infected diatom cultures and algae subjected to temperature increase. This compound plays a vital role in plant development [48], bacterial quorum sensing [49], and larval metamorphosis in ascidian *Halocynthia roretzi* [50]. The photodegradation of riboflavin can also produce it [51], and it has been found in the exometabolomes of microalgae such as *Phaeodactylum tricornutum*, *Chlamydomonas* sp. and *Desmodesmus* sp. [52]. Previous studies involving microalgae and lumichrome focus on its production by algae growth-promoting bacteria and not on the algal production of lumichrome [53]. Multiple studies also demonstrate that lumichrome supports cellular photosynthetic activity and has an overall positive effect on the growth of microalgal species such as *Phaeodactylum tricornutum*, *Chlorella sorokiniana* [53], and *Auxenochlorella protothecoides* [54]. Supporting these studies, we also suggest that high lumichrome levels correlate with high cell density and growth in diatoms, particularly at higher incubation temperatures, regardless of parasite treatment. However, further studies in *C. granii* must address whether the enhanced growth at elevated temperatures can be tied to lumichrome or if this

 doi:10.20944/preprints202410.2463.v1

compound has a role in parasite infection. No studies so far discuss the impact of temperature and interaction with parasites in lumichrome levels. A previous study in bacteria suggests that secreted lumichrome levels decline with a temperature rise and are maximum at a low temperature of 10°C [55]. However, the role of lumichrome in other marine microbes and the impact of biotic interaction with parasites herein, has not been studied thus far. Further studies are needed to clarify lumichrome's role in parasite infection.

4. Conclusions

We investigated whether temperature influences the cell abundance and metabolism of the bloom-forming diatom *C. granii* and the infectivity of its parasite *L. coscinodisci*. The increased incubation temperature modifies the alga's cell density but does not change the proportion of infected cells in the population. However, the infection rate calculated on the ratio of parasite reproductive cells (sporangia) decreases significantly at higher temperatures, indicating that this parasite might show lower reproduction at higher water temperatures. In sum, we show that the relative abundance of several metabolites can be tied to elevated temperatures, swith the up-regulation of metabolites involved in sulfur metabolism and fatty acid metabolism. We also report that metabolites of the ectoine family decrease during parasite infection but increase at higher temperatures. We highlight that changing temperature induces a specific metabolic rewiring in algal cells during parasite infection.

5. Materials and Methods

5.1. Strains and Culture Conditions for the Biological Experiments

The diatom strain RCC7046 and the parasitoid oomycete *L. coscinodisci* strain LagC19 were isolated from the same sample originating from an algal bloom at Helgoland in November 2019. The parasitoid oomycete strain was maintained in its diatom host by constant reinoculation into exponentially growing host cells every 15 days since its sampling in 2019. The diatom *C. granii* was deposited at the Roscoff Culture Collection under the strain number RCC7046 (https://roscoff-culture-collection.org/). *L. coscinodisci* and *C. granii* strains are maintained in a continuous culture by constantly propagating parasites into healthy host cultures and are available upon request. All cultures were maintained at 13°C under a light intensity of 100 mE m^2 s^{-1} following a 14h: 10h light/dark cycle. Cultures were grown in 40 mL Tissue Flasks (Sarsted) containing artificial seawater medium (ASW) [56].

5.2. Culture Conditions for the Biology Experiments

Initial inoculation from stock cultures was conducted using *C. granii* cells in the late exponential phase (initial cell density of 20 cells mL^{-1}) and was used for the algal growth experiment. Culture flasks in biological triplicates were incubated at 25°C or 13°C. Cell concentration was recorded at ten-time points over 30 days of incubation (Supplementary Figure S1). Cell density was determined by counting 1 mL culture in a Sedgwick-Rafter chamber (Pyser-SGI).

To obtain a parasite suspension containing *L. coscinodisci* zoospores, 9-day-old infected *C. granii* cultures grown at 13°C were filtered through a 20 µm cell strainer (PluriSelect) and the filtrate was used to inoculate in healthy cultures. For the infection experiment, 100 µL of a 9-day-old culture infected with *L. coscinodisci* (infection rate of 30%, cell density of 160 cells mL^{-1}) were inoculated to 40 mL of healthy cultures (cell density of 200 cells mL^{-1}). Cell density and infected cells were recorded by counting cells in 1 mL in the Sedgwick-Rafter chamber (Marienfeld, Germany). The number of healthy cells, total cell number, and number of infected cells (late infection stage sporangium) were determined under a light microscope (Leica DM 2000, Leica Microsystems, Wetzlar, Germany) in a Sedgwick-Rafter chamber (Pyser-SGI). Cultures were incubated under the two temperature regimes, 13 or 25°C, and cells were counted and inspected every two days. Images were taken using an inverted microscope (AE30, Motic) for regular checks and sub-cultivation, and a Zeiss Imager 2 (Carl Zeiss) was used to record microscopic images. This experiment was also conducted with biological

 doi:10.20944/preprints202410.2463.v1

triplicates. Raw data is presented in Supplementary Table S1. Statistical analysis and visualization of cell counts were conducted in GraphPad Prism Version 10.

5.3. Metabolic Extractions of Diatom Cultures

After seven days of incubation of the infection experiment, cultures were filtered under reduced pressure on GF/C microfiber filters (Whatman plc, Maidstone, UK) deposited on filter plates (Ø 24mm, pore size 4, glass edge, VWR International GmbH, US) in a filtration unit (Duran/pp, VWR International GmbH, Pennsylvania, US). The blank sample consisted of 40 mL of ASW medium without microbes. The GF/C filters were transferred to 2 mL safe-lock Eppendorf tubes and extracted with 1.5 mL methanol (99.8 %, anhydrous, SIGMA-ALDRICH Chemie GmbH, Munich, Germany). Cells were disrupted by ultrasonication in an ultrasonic cleaner Emmi-D280 (Emag AG, Germany) for 10 min at room temperature. The resulting mixture underwent centrifugation at 30,000 x g at 4°C for 15 minutes, facilitating debris sedimentation. Supernatants (1.2 mL) were carefully transferred to new tubes and subjected to further centrifugation for 20 minutes at 12,000 x g. The resulting supernatants were then transferred into 1.5 mL glass vials, and the solvent was evaporated using a desiccator. The dried samples were stored at -20 °C until UHPLC-HRMS analysis. Reconstitution of the dried extracts was done with 80 µL of methanol. The resulting solution was transferred into 1.5 mL safe-lock Eppendorf tubes and underwent centrifugation at 30,000 x g at 4°C as mentioned above, for 20 minutes. Subsequently, 50 µL of the resulting supernatant was transferred into LCMS glass vials containing glass inserts for subsequent analysis. To prepare the Quality Control (QC) pooled sample, 5 µL of each sample (excluding blanks) were pooled into a QC pool mix.

5.4. Chromatography

Samples for LC-MS analysis were measured with a Dionex UltiMate 3000® (Dionex, Germany) coupled to a Q-Exactive Plus Orbitrap mass spectrometer (Thermo Scientific, Bremen, Germany). Two distinct chromatographic protocols were implemented to identify a wide range of metabolites, from non-polar to polar, hence using C18 and ZIC-HILIC columns.

An Accucore C18 column (100 × 2.1 mm, particle size 2.6 µm, Thermo Scientific, US) was employed for the chromatographic separation of non-polar metabolites. Phase (A) consisted of UHPLC-grade water (2% acetonitrile, 0.1% formic acid), and phase (B) of UHPLC-grade acetonitrile (0.1% formic acid). The separation process was initiated with 100% (A) at a flow rate of 0.4 mL min^{-1}, steadily increasing gradient of (B) for 8 min to reach 100% (B), which was held for 3 min, finishing with 100% of (A) for 1 min. The sample injection volume was 10 µL.

For the chromatographic separation of polar metabolites, a SeQuant ZIC-HILIC column (150 x 2.1 mm, particle size 5 µm, Pore size 200 Å, Merck, Germany) was used, complemented by a SeQuant ZIC-HILIC guard column (20 x 2.1 mm, Merck, Germany). The phases consisted of (A) UHPLC-grade water (2% acetonitrile, 0.1% formic acid) and (B) UHPLC-grade acetonitrile (10% water, 1 mmol L^{-1} of ammonium acetate). The separation commenced with 100% (B) at a flow rate of 0.6 mL min^{-1} for 1 min, steadily increasing the gradient of (A) for 6.5 min until 25% (B) is obtained, followed by 100% B for 3.5 min and finishing with 85% (B) for 2 min. The sample injection volume used was 1 µL.

5.5. Mass Spectrometry Analysis and Data Transformation

Mass spectrometry was carried out on a Q-Exactive Plus Orbitrap (Thermo Fisher Scientific, USA). Analytes were monitored in full MS scan (Resolution 70,000, AGC target 3E+06, Maximum IT 200 ms, with polarity switch). The scan range extended from *m/z* 75 to 1,125, with a total runtime of 12 min (C18 column) or 10 min (ZIC-HILIC column).

Data-dependent MS2 (Resolution 17,500, AGC target 1E+5, Maximum IT 50 ms, loop count 5, Top N5, isolation window of 0.4 *m/z*) with a three-stepped collision energy of 15, 30, and 45 were carried out on the QC pool sample to enable metabolite identification and annotation. The MS2 measurements were acquired separately in positive and negative modes. Total Ion Chromatograms

 doi:10.20944/preprints202410.2463.v1

and Extracted Ion Chromatograms were vizualized in QualBrowser (Thermo Fisher Scientific, USA) (Supplementary Figures S2, S3)

Raw data was processed using Compound Discoverer version™ software (v 3.3.2.31; Thermo Fisher Scientific, USA) for data deconvolution and metabolite identification. The software was used to detect chromatographic peaks, perform retention time alignment using QC samples, detect unknown compounds, and group compounds across samples to generate a list of features. Each feature is characterized by a *m/z* value, retention time (min), and chemical formula annotated based on the isotopic pattern from the HRMS mass spectrum. For compound detection and fragment identification, the mass tolerances set for MS identification was 5 ppm, and the minimum peak intensity was 1E+06. The chromatographic S/N Threshold was set to 1.5 for peak detection without baseline removal. For grouping compounds and MS identification, mass tolerance was 10 ppm, with a retention time tolerance of 1 min and an S/N threshold at 5 (for Gap filling). The relative standard deviation value was set at 50, excluding features not represented in all pool samples (QC) replicates. The compound list was exported as a .csv file; the intensities were normalized based on cell density count (using the Scale Area node on Compound Discoverer) and analyzed with MetaboAnalyst 5.0. (https://www.metaboanalyst.ca/). The compound list was exported as a .csv file, and the intensities were normalized based on cell density count and analyzed with MetaboAnalyst 5.0. The cell-based normalized intensities were further log-transformed and Pareto-scaled. In MetaboAnalyst, the PCA loading plots, volcano plots, and pattern hunter analysis were used to mine significant metabolites that discriminated cell metabolic profiles from cultures grown at 25°C, 13°C, or treated with parasites. Of 1,195 features from the ZIC-HILIC dataset of *C. granii* treated by temperature and parasite, 478 were excluded based on the filter using the Interquartile range. Of 1,210 features from the C18 dataset of *C. granii* treated by temperature and parasite, 484 were excluded based on the filter using the Interquartile range. Significant features that were selected for further identification are shown in Supplementary Figures S11-S16.

5.6. Metabolite Identification

Significantly regulated metabolites identified by the statistical analysis were further investigated by acquiring MS/MS spectra using ddMS experiments on QC pool samples (Supplementary Figures S4-S10). For the identification and confirmation of significant features, the MS/MS spectra of selected ions were compared using SIRIUS (v5.8.3) and CSI: FingerID, as well as those of analytical standards. Depending on the tree fragmentation score and the percentage of CSI:FingerID tool putative identification of unknowns was performed. MS/MS raw spectra are available in the files tab. GNPS was also used to identify features not previously identified using SIRIUS and confirm the identity of the zwitterions and polar metabolites recovered from the ZIC-HILIC and C18 analysis. Assignment of identity with a confidence level was conducted using a threshold of 90% similarity obtained in SIRIUS and a minimal cosine score of 0.7 in GNPS. Analytical standards were measured to confirm the metabolites lumichrome and eicosapentaenoic acid recovered from the C18 analysis. Furthermore, DMSP, cysteinoleic acid, serine, carnitine, and acetylcarnitine were confirmed with co-injection of the QC pool sample with analytical standards. Ectoine and 2-homoectoine were identified based on spectral similarity matching with MS2 from GNPS database (http://gnps.ucsd.edu) [57]. All MS/MS spectra of our reference standards were deposited and publicly available online in the GNPS spectral libraries. The charts were made using the Metabolomics Spectrum Resolver. All spectral mirror charts had a cosine similarity score of not less than 70. Identical MS/MS spectra proved the identity of compounds from *C. granii* were identical to the reference standards. Significant metabolites that have been identified can be found in Supplementary Table S2. Co-injection studies of lumichrome and eicosapentaenoic acid with QC algal pool samples are displayed in Supplementary Figures S17-S18.

Supplementary Materials: The following supporting information can be downloaded at the website of this paper posted on Preprints.org.

Author Contributions: Conceptualization, R.O. and M.V.; methodology and data acquisition, R.O. and M.V.; data analysis, R.O. and M.V.; writing—original draft preparation, R.O. and M.V.; writing—review and editing, M.V. and G.P.; visualization, R.O. and M.V.; supervision, M.V.; project administration, M.V.; funding acquisition, M.V. All authors have read and agreed to the published version of the manuscript.

Funding: MV and GP are supported by the Deutsche Forschungsgemeinschaft (DFG, German Research Foundation), SFB1127 ChemBioSys, project number 239748522.

Data Availability Statement: The microbial strains are maintained continuously and available upon request. The datasets are available at MassIVE spectral database and the links are:
https://massive.ucsd.edu/ProteoSAFe/dataset.jsp?task=a88ae0ffac114bde8d8a9bc65e5b698b;
ftp://MSV000095877@massive.ucsd.edu; ftp://massive.ucsd.edu/v08/MSV000095877/

Conflicts of Interest: The authors declare no conflict of interest.

References

1. Deng, Y., M. Vallet, and G. Pohnert, Temporal and spatial signaling mediating the balance of the plankton microbiome. *Annual Review of Marine Science*, **2022**. *14*(1): p. 239-260.
2. Cirri, E. and G. Pohnert, Algae–bacteria interactions that balance the planktonic microbiome. *New Phytologist*, **2019**. *223*(1): p. 100-106.
3. Brisson, V., et al., Dynamic *Phaeodactylum tricornutum* exometabolites shape surrounding bacterial communities. *New Phytologist*, **2023**. *239*(4): p. 1420-1433.
4. Brown, E.R., et al., Chemical ecology of the marine plankton. *Natural Product Reports*, **2019**. *36*(8): p. 1093-1116.
5. Egan, S., et al., The seaweed holobiont: understanding seaweed–bacteria interactions. *FEMS Microbiology Reviews*, **2013**. *37*(3): p. 462-476.
6. Chambouvet, A., et al., Control of toxic marine dinoflagellate blooms by serial parasitic killers. *Science*, **2008**. *322*(5905): p. 1254-1257.
7. Ilicic, D. and H.-P. Grossart, Basal parasitic fungi in marine food webs: A mystery yet to unravel. *Journal of Fungi*, **2022**. *8*(2): p. 114.
8. Vallet, M., Chemical ecology of plankton parasites. *Botanica Marina*, **2024**.
9. Ismail, S., et al., Temperature and intraspecific variation affect host–parasite interactions. *Oecologia*, **2023**.
10. Deppeler, S.L. and A.T. Davidson, Southern ocean phytoplankton in a changing climate. *Frontiers in Marine Science*, **2017**. *4*.
11. Basu, S. and K.R.M. Mackey, Phytoplankton as key mediators of the biological carbon pump: their responses to a changing climate. *Sustainability*, **2018**. *10*(3): p. 869.
12. Godwin, S.C., et al., Increasing temperatures accentuate negative fitness consequences of a marine parasite. *Scientific Reports*, **2020**. *10*(1): p. 18467.
13. Hector, T.E., et al., Symbiosis and host responses to heating. *Trends in Ecology & Evolution*, **2022**. *37*(7): p. 611-624.
14. Schampera, C., et al., Parasites do not adapt to elevated temperature, as evidenced from experimental evolution of a phytoplankton–fungus system. *Biology Letters*, **2022**. *18*(2): p. 20210560.
15. Wood, C.L., et al., A reconstruction of parasite burden reveals one century of climate-associated parasite decline. *Proceedings of the National Academy of Sciences*, **2023**. *120*(3): p. e2211903120.
16. Vallet, M., et al., The oomycete *Lagenisma coscinodisci* hijacks host alkaloid synthesis during infection of a marine diatom. *Nature Communications*, **2019**. *10*(1): p. 4938.
17. Vallet, M., et al., Single-cell metabolome profiling for phenotyping parasitic diseases in phytoplankton. *Frontiers in Analytical Science*, **2023**. *2*.
18. Kafsack, B.F. and M. Llinás, Eating at the table of another: metabolomics of host-parasite interactions. *Cell Host Microbe*, **2010**. *7*(2): p. 90-9.
19. Hildebrand, M., S.J.L. Lerch, and R.P. Shrestha, Understanding diatom cell wall silicification—Moving forward. *Frontiers in Marine Science*, **2018**. *5*.
20. Kuhlisch, C. and G. Pohnert, Metabolomics in chemical ecology. *Natural Product Reports*, **2015**. *32*(7): p. 937-955.
21. Pohnert, G. and W. Boland, The oxylipin chemistry of attraction and defense in brown algae and diatoms. *Natural Product Reports*, **2002**. *19*(1): p. 108-122.
22. OBIS. Ocean Biodiversity Information System. 2024; Available from: www.obis.org.
23. Huang, H., et al., Genetic diversity and geographical distribution of the Red Tide species *Coscinodiscus granii* revealed using a high-resolution molecular marker. *Microorganisms*, **2022**. *10*(10): p. 2028.
24. Holfeld, H., Relative abundance, rate of increase, and fungal infections of freshwater phytoplankton. *Journal of Plankton Research*, **2000**. *22*(5): p. 987-995.

25. Schmitt, M., et al., Temperature affects the biological control of dinoflagellates by the generalist parasitoid *Parvilucifera rostrata*. *Microorganisms*, **2022**. *10*(2): p. 385.
26. Wang, G., et al., Robust warming pattern of global subtropical oceans and its mechanism. *Journal of Climate*, **2015**. *28*(21): p. 8574-8584.
27. Thomas, M.K., et al., A global pattern of thermal adaptation in marine phytoplankton. *Science*, **2012**. *338*(6110): p. 1085-1088.
28. Wetsteyn, L.P.M.J. and L. Peperzak, Field observations in the Oosterschelde (The Netherlands) on *Coscinodiscus concinnus* and *Coscinodiscus granii* (Bacillariophyceae) infected by the marine fungus *Lagenisma coscinodisci* (Oomycetes). *Hydrobiological Bulletin*, **1991**. *25*(1): p. 15-21.
29. Liang, Y., et al., Molecular mechanisms of temperature acclimation and adaptation in marine diatoms. *The ISME Journal*, **2019**. *13*(10): p. 2415-2425.
30. Case, R.J., et al., Temperature induced bacterial virulence and bleaching disease in a chemically defended marine macroalga. *Environmental Microbiology*, **2011**. *13*(2): p. 529-537.
31. Demory, D., et al., Temperature is a key factor in *Micromonas*–virus interactions. *The ISME Journal*, **2017**. *11*(3): p. 601-612.
32. Azizah, M. and G. Pohnert, Orchestrated response of intracellular zwitterionic metabolites in stress adaptation of the halophilic heterotrophic bacterium *Pelagibaca bermudensis*. *Mar Drugs*, **2022**. *20*(11).
33. Garcés, E., et al., Host-released dimethylsulphide activates the dinoflagellate parasitoid *Parvilucifera sinerae*. *The ISME Journal*, **2013**. *7*(5): p. 1065-1068.
34. Barak-Gavish, N., et al., Bacterial virulence against an oceanic bloom-forming phytoplankter is mediated by algal DMSP. *Science Advances*, **2018**. *4*(10): p. eaau5716.
35. Seymour, J.R., et al., Chemoattraction to dimethylsulfoniopropionate throughout the marine microbial food web. *Science*, **2010**. *329*(5989): p. 342-345.
36. Garren, M., et al., A bacterial pathogen uses dimethylsulfoniopropionate as a cue to target heat-stressed corals. *The ISME Journal*, **2013**. *8*(5): p. 999-1007.
37. Fenizia, S., J. Weissflog, and G. Pohnert, Cysteinolic acid is a widely distributed compatible solute of marine microalgae. *Marine Drugs*, **2021**. *19*(12): p. 683.
38. Azizah, M. and G. Pohnert, 2-Homoectoine: An additional member of the ectoine family from phyto- and bacterioplankton involved in osmoadaptation. *Journal of Natural Products*, **2024**. *87*(1): p. 50-57.
39. Khozin-Goldberg, I., Lipid metabolism in microalgae, in *The Physiology of Microalgae*, M.A. Borowitzka, J. Beardall, and J.A. Raven, Editors. 2016, Springer International Publishing: Cham. p. 413-484.
40. Nikitashina, V., D. Stettin, and G. Pohnert, Metabolic adaptation of diatoms to hypersalinity. *Phytochemistry*, **2022**. *201*: p. 113267.
41. Imazaki, A., et al., Contribution of peroxisomes to secondary metabolism and pathogenicity in the fungal plant pathogen *Alternaria alternata*. *Eukaryotic Cell*, **2010**. *9*(5): p. 682-694.
42. Blasio, M. and S. Balzano, Fatty acids derivatives from eukaryotic microalgae, pathways and potential applications. *Front Microbiol*, **2021**. *12*: p. 718933.
43. Wen, Z.-Y. and F. Chen, Application of statistically-based experimental designs for the optimization of eicosapentaenoic acid production by the diatom *Nitzschia laevis*. *Biotechnology and Bioengineering*, **2001**. *75*(2): p. 159-169.
44. Hu, H. and K. Gao, Response of growth and fatty acid compositions of *Nannochloropsis* sp. to environmental factors under elevated CO_2 concentration. *Biotechnology Letters*, **2006**. *28*(13): p. 987-992.
45. Yodsuwan, N., S. Sawayama, and S. Sirisansaneeyakul, Effect of nitrogen concentration on growth, lipid production and fatty acid profiles of the marine diatom *Phaeodactylum tricornutum*. *Agriculture and Natural Resources*, **2017**. *51*(3): p. 190-197.
46. B, J., et al., Nitrogen repletion favors cellular metabolism and improves eicosapentaenoic acid production in the marine microalga *Isochrysis* sp. CASA CC 101. *Algal Research*, **2020**. *47*: p. 101877.
47. Decelle, J., et al., Intracellular development and impact of a marine eukaryotic parasite on its zombified microalgal host. *The ISME Journal*, **2022**. *16*(10): p. 2348-2359.
48. Dakora, F.D., V. Matiru, and A.S. Kanu, Rhizosphere ecology of lumichrome and riboflavin, two bacterial signal molecules eliciting developmental changes in plants. *Frontiers in Plant Science*, **2015**. *6*.
49. Rajamani, S., et al., The vitamin riboflavin and its derivative lumichrome activate the LasR bacterial quorum-sensing receptor. *Molecular Plant-Microbe Interactions®*, **2008**. *21*(9): p. 1184-1192.
50. Tsukamoto, S., et al., Lumichrome. *European Journal of Biochemistry*, **1999**. *264*(3): p. 785-789.
51. Ahmad, I., et al., Photolysis of riboflavin in aqueous solution: a kinetic study. *International Journal of Pharmaceutics*, **2004**. *280*(1): p. 199-208.
52. Brisson, V., et al., Identification of effector metabolites using exometabolite profiling of diverse microalgae. *mSystems*, **2021**. *6*(6): p. e00835-21.
53. Lopez, B.R., et al., Riboflavin and lumichrome exuded by the bacterium *Azospirillum brasilense* promote growth and changes in metabolites in *Chlorella sorokiniana* under autotrophic conditions. *Algal Research*, **2019**. *44*: p. 101696.

 doi:10.20944/preprints202410.2463.v1

54. Peng, H., L.E. de- Bashan, and B.T. Higgins, Comparison of algae growth and symbiotic mechanisms in the presence of plant growth promoting bacteria and non-plant growth promoting bacteria. *Algal Research*, **2021**. *53*: p. 102156.
55. Kanu, S. and F.D. Dakora, Thin-layer chromatographic analysis of lumichrome, riboflavin and indole acetic acid in cell-free culture filtrate of *Psoralea nodule* bacteria grown at different pH, salinity and temperature regimes. *Symbiosis*, **2009**. *48*(1): p. 173-181.
56. Maier, I. and M. Calenberg, Effect of extracellular Ca2+ and Ca2+-antagonists on the movement and chemoorientation of male gametes of *Ectocarpus siliculosus* (Phaeophyceae). *Botanica Acta*, **1994**. *107*(6): p. 451-460.
57. Wang, M., et al., Sharing and community curation of mass spectrometry data with Global Natural Products Social Molecular Networking. *Nature Biotechnology*, **2016**. *34*(8): p. 828-837.